Letter

optica

Optoelectronic feedback with a monolithically integrated quantum dot micropillar detector and laser assembly

PIERCE MUNNELLY,[1] BENJAMIN LINGNAU,[2] MATTHIAS M. KAROW,[1] TOBIAS HEINDEL,[1] MARTIN KAMP,[3] SVEN HÖFLING,[3,4] KATHY LÜDGE,[2] CHRISTIAN SCHNEIDER,[3] AND STEPHAN REITZENSTEIN[1,*]

[1]*Institute of Solid State Physics, Technische Universität Berlin, 10623 Berlin, Germany*
[2]*Institute for Theoretical Physics, Technische Universität Berlin, 10623 Berlin, Germany*
[3]*Department of Technische Physik, Universität Würzburg, 97074 Würzburg, Germany*
[4]*School of Physics and Astronomy, University of St Andrews, St Andrews KY16 9SS, United Kingdom*
**Corresponding author: stephan.reitzenstein@physik.tu-berlin.de*

Received XX Month XXXX; revised XX Month, XXXX; accepted XX Month XXXX; posted XX Month XXXX (Doc. ID XXXXX); published XX Month XXXX

An integrated optoelectronic feedback system based on semiconductor quantum dot-micropillars is presented. The device consists of an electrically driven microlaser optically coupled to monolithically integrated photodetectors. Via the external amplification and reinjection of the detector photocurrent into the microlaser, self-pulsing in the optoelectronic signal is observed. The feedback-induced self-pulsing is explained qualitatively by a rate equation model, which considers the thermally induced shift in the gain of the laser during pulsing and a Gaussian white-noise term for spontaneous emission. The results show promise for exploring chaos in ultra-compact nanophotonic systems and for technological approaches towards chaos-based secure communication, random number generation, and self-pulsing single photon sources on a highly integrated semiconductor platform.

OCIS codes: *(230.5160) Photodetectors; (130.3120) Integrated optics devices; (140.3945) Microcavities; (130.3060) Infrared; (230.5590) Quantum-well, -wire and -dot devices.*

http://dx.doi.org/10.1364/optica.xx.xxxxxx

Semiconductor lasers undergoing feedback are known to demonstrate rich nonlinear dynamics and have provoked much research in the fields of chaos, synchronization and secure communication [1—3]. The manifestations of feedback in lasers can be either detrimental or beneficial to device performance. For instance, optical feedback caused by unwanted reflections at facets is known to cause data distortion in laser-based optoelectronic communication [4]; on the other hand, low optical feedback levels can be exploited, e.g., to reduce laser linewidths [5] and pulse jitter for better signal integrity [6—8]. In particular, optoelectronic feedback, where the laser light is converted to an electrical signal which incoherently modulates the carrier density within the laser [9], allows one to explore routes to chaotic dynamics [10]. It has also had significant technological impact as it has been shown to be useful for the suppression of unwanted bistabilities in directly-modulated semiconductor lasers [11].

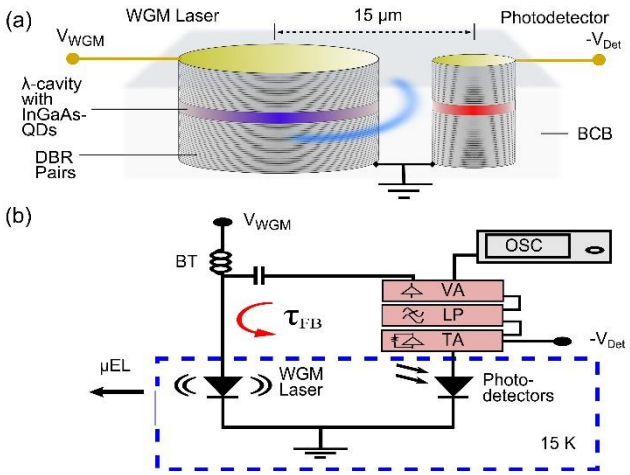

Fig. 1. Sample layout (a) and sketch of the setup for the optoelectronic feedback experiment (b). As illustrated in panel (b) the extracted photocurrent is amplified by the transimpedance amplifier (TA), and is then passed through a 2 MHz-bandwidth low-pass filter (LP) before being amplified at the main voltage amplifier (VA). The output voltage of the VA was coupled into the laser channel via a bias-T (BT) and simultaneously monitored on an oscilloscope (OSC) via a second output port. Scattered laser light was analyzed at a micro-electroluminescence (µEL) spectroscopy setup for optical measurements.

Quantum dot (QD) -based micropillar lasers exhibit low threshold currents thanks to their small mode volumes and high Q-factors, and can serve as excellent testbeds for studying the effects of feedback on lasing at ultra-low light levels in the cavity-quantum electrodynamic (cQED) regime [12,13]. Apart from generating light, electrically

contacted QD-micropillars can also be applied to detect photons down to the single-QD regime of cQED [14,15], making them applicable as light-sensitive devices for on-chip quantum optical experiments [16—18].

In this report, we present interdisciplinary work in which we combine the above mentioned fields in an ultra-compact optoelectronic feedback scheme, which is based on a monolithically integrated microlaser-microdetector assembly. Here, an electrically driven whispering gallery mode (WGM) micropillar laser creates photocurrent within negatively-biased QD micropillar detectors displaced 15 μm from the WGM microlaser. The extracted photocurrent is amplified within a 2 MHz bandwidth, and fed back to the microlaser within the integrated microlaser-microdetector optoelectronic feedback concept. This feedback leads to a significant modification of the laser behavior and results in the onset of dynamical features in the emission intensity over a certain range of laser bias currents. Clear indications of feedback influencing the laser emission are observed, such as undulations in the input-output curve, and periodic pulsing of the laser's optical output. To describe the observed effects we apply a rate equation model with temperature-induced gain changes and a stochastic noise source. The fact that feedback effects can be observed at MHz-frequencies opens attractive avenues of research into nonlinear dynamics and may also lead to new insights into slow-timescale chaos. Future applications in quantum optics such as on-chip triggering of single photon sources can also be foreseen.

A schematic of the sample layout can be seen in Fig. 1 (a). The larger, 8 μm-diameter WGM micropillar laser is monolithically integrated on the same chip as a group of five surrounding micropillars with smaller diameter (2 μm) which, when reverse-biased, serve as photodetectors [18]. Here, an assembly of five detector-pillars was chosen to increase the photocurrent generated by the common WGM microlaser. The group of photodetectors form a semicircle contacted in parallel with each other (one such detector is shown in Fig. 1 (a) for clarity), and the active region of the detectors lies within the same plane as the radial WGM laser emission [16]. The radial separation between the central microlaser and the semicircular photodetector arrangement is 15 μm. This geometrical configuration leads to a rather low detection efficiency, which in combination with the external amplifier is nevertheless sufficient to observe pronounced feedback effects in our proof-of-principle work. The lasers and detectors are constructed from a planar microcavity structure grown by molecular-beam epitaxy on an n-doped (100)-oriented GaAs substrate. A single layer of self-organized InGaAs quantum dots (area density $\sim 10^9$ cm^{-2}) is embedded within a pin-doped distributed Bragg reflector (DBR) cavity. For more details in the DBR layer design we refer to [17]. Cylindrical micropillar-cavities are realized via electron-beam lithography and reactive-ion plasma etching, and the etched structure is subsequently planarized using the polymer bencocyclobutene (BCB). Finally, individual gold contacts are evaporated onto the p-doped upper part of the micropillar cavities for electrical pumping of the lasers and extraction of the photocurrent from the detectors [19].

Fig. 1 (b) illustrates the setup used for the optoelectronic feedback experiment. Here, a photocurrent generated by the microlaser within the group of detectors was extracted, amplified and fed back to the laser. The sample was held at 15 K within a liquid helium-flow cryostat. A forward bias voltage, V_{WGM}, was applied to the WGM microlaser whose stray light scattered from the detectors into the vertical direction was collected by an objective (numerical aperture 0.42) and analyzed with a micro-electroluminescence (μEL) spectroscopy setup with a spectral resolution of 85 μeV. The transimpedance amplifier (TA) with a bandwidth of 20 MHz delivered a variable detector bias voltage V_{Det} to the detector-group, which served to extract the photocurrent (0.2 - 0.3 μA per pillar on average at a laser current of 188 μA) generated by the microlaser under continuous-wave operation (see below for more details). In order to increase the signal-to-noise ratio (SNR) in measuring photocurrents << 1 μA and to exclude external radio frequencies from the circuit, we limited the measurement bandwidth to 2 MHz by low-pass filter (LP) with a stopband attenuation greater than 60 dB. The preamplified, filtered signal was passed through a larger-gain voltage amplifier (VA) with 200 MHz bandwidth, with the overall amplification of the circuit being 0.79 V/μA and a maximum output voltage from the VA of 2.75 V peak-to-peak. This amplified voltage was then coupled back into the WGM microlaser through a bias-tee (BT) with a high-pass cutoff frequency of ~ 10 Hz. The VA has a second output, which allowed us to monitor the amplified time-varying photocurrent signal in realtime with an oscilloscope (OSC) which has a 2-GHz bandwidth. The two-stage external amplifier configuration was designed with the best SNR achievable and was necessary as in the present device design, the photocurrent alone was not enough to modify the gain directly. The TA has an input-referred noise density of 5 pAHz^{-2} at 20 MHz measured with a 40 pF input capacitance, which is the total estimated capacitance of our sample and cabling within the cryostat. The effective round-trip time τ_{FB} of the feedback circuit was measured to be (610 ± 3) ns in an open-loop configuration with the sample removed.

We first characterized the emission properties of the integrated WGM microlaser without feedback. The laser was driven in forward bias and scattered light was collected and analyzed with a μEL spectroscopy setup (see [17] for details of the setup). Fig. 2 (a) shows the input-output characteristic curve of an 8 μm-diameter WGM laser obtained by fitting the μEL spectra with a Voigt function, with the onset of lasing evidenced by the sudden drop in the fitted emission linewidth (full-width at half maximum, FWHM) of the laser mode to the setup's spectral resolution limit. A linear fit to the integrated intensity of the laser mode allowed for a threshold current of 40 μA (at 4.3 V) to be determined. An exemplary spectrum of the single-mode microlaser driven at 240 μA is shown in the inset of Fig. 2 (a). A FWHM of the laser mode as low as (1.8 ± 0.1) μeV was measured at this current using a Fabry-Pérot interferometer.

Next, we investigate the microlaser-microdetector system in the feedback configuration outlined in Fig. 1(b). The feedback consists of a positive voltage coupled into the laser via the p-contact. Although the dark current is notable relative to the photocurrent for the feedback experiments performed here, it is only the time-varying current which was detected by the TA and passed as an amplified voltage to the laser through the BT. The bias voltage on the detectors, and thus the dark current, remained constant during the recording of each data set. The electrical coupling between the laser and the detector via the common substrate was found to be negligible. In the presence of feedback, the behavior of the microlaser is markedly different to the case without feedback. This is highlighted in Fig. 2(c) by a comparison between the input-output characteristics of the laser mode with feedback (light red circles) and without feedback (solid black circles) below DC threshold I_{thr}. In the semi-logarithmic scaling used here, pronounced undulations in the integrated intensity of the laser mode can be seen as the bias laser current is increased in the presence of optoelectronic feedback. These undulations are indicative of non-linear modulation of the laser current due to feedback. The increased laser-mode visibility at such low bias currents can be attributed to the following: spontaneous emission-induced photocurrent is converted to a time-varying voltage delivered to the laser which, together with electronic noise, has an initial peak-to-peak magnitude of 900 mV at V_{WGM} = 1.0 V and V_{Det} = -10.3 V. Consequently, it modulates the laser current and leads to laser emission even below the nominal DC threshold current. Further, there is a blue-shift in the QD gain maximum under AC and DC excitation compared with the purely DC case which better feeds the laser mode. Fig. 2 (d) demonstrates this with the appearance of the laser mode at 1.448 eV in the laser spectrum at DC bias currents as low as 4.8 μA, far below the DC threshold value of 40 μA.

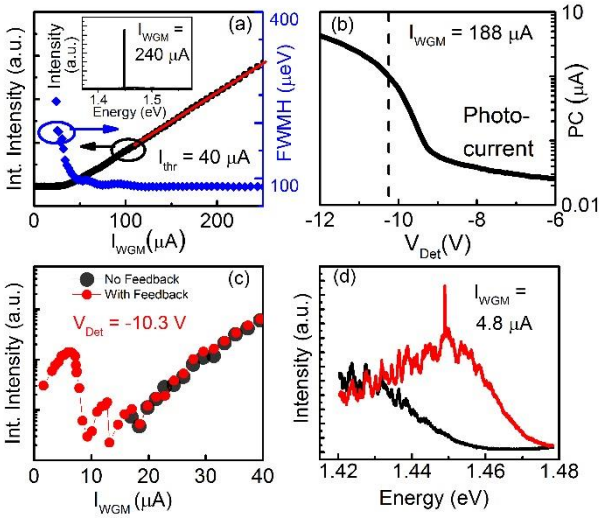

Fig. 2. WGM laser and photodetector feedback device characterization at 15 K. (a) Input-output curve and full-width at half-maximum (FWHM) of the laser emission from an 8 μm-diameter electrically driven WGM laser without feedback and a threshold current I_{thr} of 40 μA. The inset shows a μEL spectrum of the single-mode laser without feedback at a current I_{WGM} = 240 μA. (b) Photocurrent (PC) extracted from the detectors as a function of detector bias V_{Det} at a constant laser current of I_{WGM} = 188 μA (at 7.3 V) without feedback. The vertical dashed line indicates the detector bias range $V_{Det} \in$ {-10.2 V, -10.3 V} for which the optoelectronic feedback experiment was carried out. The respective PC is approximately 1 μA. (c) Input-output curves in semi-logarithmic scaling of the 8 μm laser below DC threshold with (red, light circles) and without (black, solid circles) feedback (fb) at V_{Det} = -10.3 V. (d) μEL spectra of the laser with and without feedback.

Next, we analyze the dynamics of the laser mode emission under optoelectronic feedback. Fig. 3 (a) and (b) show the experimental and simulated feedback-induced amplifier output time traces, respectively, while panels (c) and (d) show their respective Fast-Fourier transforms within the bandpass of the setup. In Fig. 3 (a), the laser bias was increased in 0.5 V steps (values of I_{WGM} relative to the DC threshold I_{thr} shown above each waveform) while the detector bias was held constant at -10.2 V. When the laser is biased at $I_{WGM}/I_{thr} = 1.5\times10^{-4}$, the amplitude of the VA output is ~600 mV peak-to-peak. At this low value of laser current, only spontaneous emission is responsible for the photocurrent created in the detectors and the WGM laser has not yet begun to lase. As the relative bias current increases to 0.03, the laser mode becomes visible in the emission spectrum and subsequent photocurrent amplification becomes strong enough to generate self-sustained pulses in the amplifier output with a maximum peak-to-peak amplitude of ~2.3 V at I_{WGM}/I_{thr} = 0.09. The slow pulses in Fig. 3 (a) vary in amplitude and yet are very regular in separation with a period of ~16 kHz at I_{WGM}/I_{thr} = 0.03, increasing with the relative bias current to ~28 kHz at I_{WGM}/I_{thr} = 0.09. This kHz envelope contains a faster oscillation at a frequency close to $1/\tau_{FB}$, corresponding to the time required for pulses of laser light to be converted into photocurrent, processed by the electronics and passed back into the laser. This is evidenced by the second dominant frequency at 1.54 MHz (corresponding to τ_{FB} = 0.65 μs) appearing in the power spectrum of Fig. 3 (c), becoming significant only after the onset of lasing. This frequency becomes more prominent as the laser bias is increased throughout the series until it falls off accompanied by the vanishing of the kHz-envelope. Long time-scale periodicity as well as chaos can emerge simultaneously in optoelectronic feedback systems [20], although the electronic bandwidth of our setup (2 MHz) precludes the observation of any dynamics on the timescale of the relaxation oscillations (GHz), which are where chaotic dynamics are most commonly observed under delayed feedback in the literature. Chaotic pulsing of semiconductor lasers under optoelectronic feedback has also been observed at much slower timescales compared to the relaxation-oscillation frequency when an additional bandwidth limitation is introduced to the feedback signal [10,21]. Here however, we observe an additional prominent oscillation at a few kHz, which cannot be explained by the bandpass-filtering of the feedback signal. Instead, we attribute this slow dynamic timescale to thermal effects, which are known to have characteristic timescales in the order of μs, and which have previously been shown to induce slow dynamics in semiconductor lasers [22]. The origin of this microsecond timescale pulsing is attributed to the thermal shift of the gain spectrum and the related dynamical change of I_{thr} as the current in the laser varies. Ohmic heating due to such voltage pulses was verified to cause the laser mode to shift by 100 μeV, which is related to a temperature change of about 20 K [23]. A bi-exponential decay was measured in a separate experiment to explore the dynamical features of this dependence.

In order to describe the optoelectronic feedback dynamics in our integrated microsystem, we used a rate-equations model to simulate the input-output characteristics and dynamics of the WGM laser mode emission under optoelectronic feedback. Our theoretical description goes beyond existing optoelectronic feedback models by including temperature-induced gain changes as dynamic variables. The model consists of the following equations:

$$\frac{d}{dt}S(t) = \left[(G(t)N(t) - 1) - \frac{1}{\tau_S}\right]S(t) + \sqrt{\beta\frac{N(t)}{\tau_N}}\xi_{sp} \quad \textbf{(1)}$$

$$\frac{d}{dt}N(t) = \frac{I(t)-N(t)}{\tau_N} - [G(t)N(t) - 1]S(t) \quad \textbf{(2)}$$

$$\frac{d}{dt}T_i(t) = \frac{1}{\tau_{T_i}}\left[C_{S_i}S(t) - T_i(t)\right] \quad \textbf{(3)}$$

$$\frac{d}{dt}I_{FB}(t) = \frac{2\pi}{\tau_{lp}}[\kappa S(t - \tau_{FB}) - I_{FB}(t)]. \quad \textbf{(4)}$$

The equations describe time-dependent values for a laser with a cavity photon number S(t), a normalized carrier number $N(t)$, a normalized temperature rise above ambient $T = T_1 + T_2$ and a feedback current $I_{FB}(t)$. The strength of the feedback is given by κ. $G(t)$ is the normalized optical gain and has a dependence on the temperature via $G(t)=1/(1+T_1+T_2)$, accounting for a decrease in gain with the local increase in temperature caused by an increase in $S(t)$. The latter is an essential effect in order to describe the experimentally observed dynamics under feedback. The total current $I(t)$ consists of the AC feedback current $I_{FB}(t)$ and the DC bias current I_{WGM} via $I(t) = I_{WGM} + min(I_{FB}(t), I_{FB}^{max})$, which constrains the current in the equations to the maximum output of the electronics used in the experiment. The effect of the low-pass filter is approximated as first-order and is implemented in the model by the time constant τ_{lp}. The delay time is τ_{FB} as indicated in Fig. 1 (b) and represents the effective round-trip time of the signal from photodetector to microlaser. τ_S is the cavity photon lifetime, and the effective carrier lifetime τ_N includes the carrier scattering time of the refilling from reservoir states. The dimensionless fit parameters C_{Si} determine the rates at which the temperature is driven by the photon number, and the two timescales τ_{T1} and τ_{T2} are of a bi-exponential dependence with which the gain recovers. The timescales were experimentally determined by a time-resolved detection of the cavity mode's energy, which is indicative of the local temperature of the microlaser. Spontaneous emission is included by the stochastic normalized Gaussian white noise source ξ_{sp}, and β is the spontaneous emission coupling factor. The value of the parameters used in the simulations are displayed in Table 1. The dynamic simulations shown in Fig. 3 (b) and (d) are found to qualitatively reproduce the experimental current dependence, i.e. the appearance of a slow kHz modulation within a small current range. The slow modulation is found to disappear when neglecting the temperature change in the model, clearly showing the importance of thermal effects in the observed dynamics. The discrepancy between experiment and simulation in the values for the current at which the dynamics begin is explained in part by the reduction in threshold under DC and AC excitation compared to the purely DC case as discussed above, which was not taken into account.

Table 1. Parameters used in the rate-equation simulation Eqs. (1) – (4) for optoelectronic feedback.

Parameter	Value	Parameter	Value
τ_S	10 ps	τ_{FB}	610 ns
τ_N	10 ps	τ_p	500 ns
τ_{T1}	6 µs	I^{max}_{FB}	240
τ_{T2}	1 µs	β	0.01
C_{S1}	0.08	I^{theory}_{thr}	100
C_{S2}	0.0125	κ	8

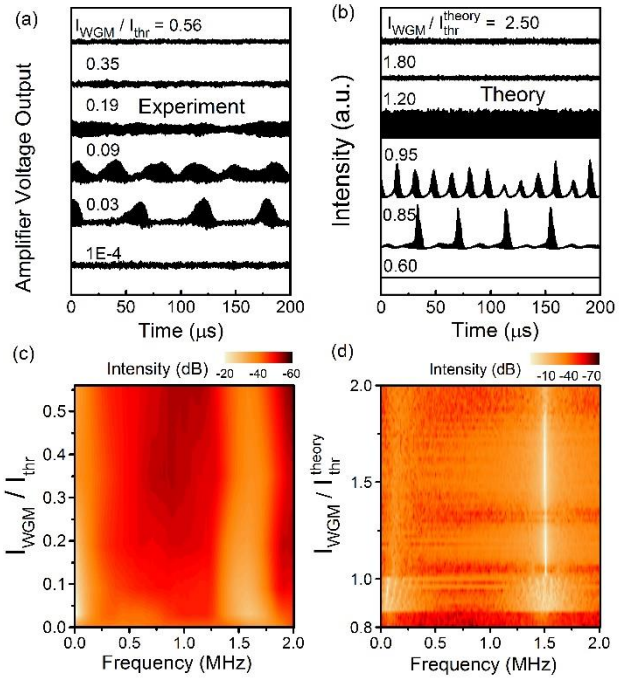

Fig. 3. Experimental and simulated time traces and power spectra for WGM microlaser emission under optoelectronic feedback. (a) Time traces of the feedback-induced laser emission with V_{Det} = -10.2 V for varying relative bias current, as experimentally recorded on the oscilloscope in Fig. 1. (b) The simulated time traces of the laser mode intensity during feedback for increasing relative bias current. (c), (d) The corresponding spectral components of the time series in (a) and (b) respectively, within the 2 MHz bandwidth allowed by the low-pass filter.

In conclusion, optoelectronic feedback using a QD-based, monolithically integrated microlaser-microdetector assembly has been realized and investigated experimentally as well as theoretically. Self-pulsing of the microlaser was observed over a narrow range of laser biases, and the system was modelled with rate equations in dependence of cavity photon number, charge carrier number and a temperature dependence of the microlaser gain qualitatively reproducing the experimental results. We find that the inclusion of thermal effects is necessary to describe the observed µs modulation of the laser output under feedback. With further development, our platform could be employed for diverse applications such as tuning the external cavity geometry to match the laser excitation, forming an integrated resonant detection device with a higher efficiency and potential use for in-situ monitoring. Integration of amplifier electronics on the same chip would comprise a truly self-contained, on-chip feedback system for compact chaotically secure communication [24] or for an array of self-pulsed single-photon source when utilizing one or more external micropillars as a quantum light emitter instead of as a photodetector. Also, a network of nonlinear oscillators could be conceived for studying complex nonlinear dynamics [25]. Further work is required to optimize the contact layout and reduce parasitic capacitances for an increase in bandwidth in order to compete with other feedback schemes utilizing a wholly off-chip detection method. Additional improvements can be made to the detector geometry to increase the extracted photocurrent. For instance, deformed resonator geometries such as the Limaçon of Pascal can be exploited for laser emission preferentially in the direction of the detectors [26].

Funding.

The research leading to these results has received funding from the European Research Council under the European Union's Seventh Framework ERC Grant Agreement No. 615613, from the German Research Foundation via the projects RE2974/9-1, SCHN1376/1-1, and the collaborative research center CRC787.

Acknowledgment.

Expert sample preparation by M. Emmerling is gratefully acknowledged.

REFERENCES

1. M. C. Soriano, J. García-Ojalvo, C. R. Mirasso and I. Fischer, Rev. Mod. Phys. **85**, 421 (2013).
2. R. Lang and K. Kobayashi, IEEE J. Quantum Electron. **16**, 3 (1980).
3. J. Ohtsubo, Opt. Rev. **6**, 1 (1999).
4. O. Hirota and Y. Suematsu, IEEE J. Quantum Electron. **15**, 3 (1979).
5. E. Patzak, H. Olesen, A. Sugimura, S. Saito, and T. Mukai, Electron. Lett. **19**, 22 (1983).
6. D. Arsenijević, M. Kleinert and D. Bimberg, Appl. Phys. Lett. **103**, 231101 (2013).
7. L. C. Jaurigue, O. Nikiforov, E. Schöll, S. Breuer and K. Lüdge, Phys. Rev. E **93**, 2 (2016).
8. K. Kobayashi, IEICE Trans. E**59**, 12 (1976).
9. G. Giacomelli, M. Calzavara and F. T. Arecchi, Opt. Commun. **74**, 1,2 (1989).
10. S. Tang and J. M. Liu, IEEE J. Quantum Electron. **37**, 3 (2001).
11. S. Rajesh and V.M. Nandakumaran, Physica D **213**, 113 (2006).
12. F. Albert, C. Hopfmann, S. Reitzenstein, C. Schneider, S. Höfling, L. Worschech, M. Kamp, W. Kinzel, A. Forchel, and I. Kanter, Nat. Commun. **2**, 366 (2011).
13. C. Hopfmann, F. Albert, C. Schneider, S. Höfling, M. Kamp, A. Forchel, I. Kantner, and S. Reitzenstein, New J. Phys. **15**, 025030 (2013).
14. C. Kistner, S. Reitzenstein, C. Schneider, S. Höfling and A. Forchel, Appl. Phys. Lett. **94,** 221103 (2009).
15. P. Gold, M. Gschrey, C. Schneider, S. Höfling, A. Forchel, M. Kamp and S. Reitzenstein, Phys. Rev. B **86,** 161301(R) (2012).
16. E. Stock, F. Albert, C. Hopfmann, M. Lermer, C. Schneider, S. Höfling, A. Forchel, M. Kamp, and S. Reitzenstein, Adv. Mater. **25**, 707 (2013).
17. P. Munnelly, T. Heindel, M. M. Karow, S. Höfling, M. Kamp, C. Schneider, and S. Reitzenstein, IEEE J. Sel. Top. Quantum Electron. **21**, 681 (2015).
18. M. M. Karow, P. Munnelly, T. Heindel, M. Kamp, S. Höfling, C. Schneider, and S. Reitzenstein, Appl. Phys. Lett. **108**, 081110 (2016).
19. C. Böckler, S. Reitzenstein, C. Kistner, R. Debusmann, A. Löffler, T. Kida, S. Höfling, A. Forchel, L. Grenouillet, J. Claudon and J. M. Gérard, Appl. Phys. Lett. **92**, 091107 (2008).
20. Y. C. Kouomou, P. Colet, L. Larger, and N. Gastaud, Phys. Rev. Lett. **95**, 203903 (2005).
21. K. Al-Naimee, F. Marino, M. Ciszak, R. Meucci, and F. T. Arecchi, New J. Phys. **11**, 073022 (2009).
22. E.A. Viktorov and T. Erneux, Phys. Rev. E **90**, 052914 (2014).
23. J. P. Reithmaier, G. Sęk, A. Löffler, C. Hofmann, S. Kuhn, S. Reitzenstein, L.V. Keldysh, V. D. Kulakovskii, T. L. Reinecke and A. Forchel, Nature **432**, 197 (2004).
24. M. Sciamanna and K. A. Shore, Nat. Photonics **9**, 151 (2015).
25. S. Tang, R. Vicente, M. C. Chiang, C. R. Mirasso and J.-M. Liu, IEEE J. Sel. Top. Quantum Electron. **10**, 5 (2004).
26. F. Albert, C. Hopfmann, A. Eberspächer, F. Arnold, M. Emmerling, C. Schneider, S. Höfling, A. Forchel, M. Kamp, J. Wiersig and S. Reitzenstein, Appl. Phys. Lett. **101**, 021116 (2012).

1. M. C. Soriano, J. García-Ojalvo, C. R. Mirasso and I. Fischer, "Complex photonics: Dynamics and applications of delay-coupled semiconductors lasers," Rev. Mod. Phys. **85**, 421 (2013).
2. R. Lang and K. Kobayashi, "External optical feedback effects on semiconductor injection laser properties," IEEE J. Quantum Electron. **16**, 3 (1980)
3. J. Ohtsubo, "Feedback induced instability and chaos in semiconductor lasers and their applications," Opt. Rev. **6**, 1 (1999).
4. O. Hirota and Y. Suematsu, "Noise properties of injection lasers due to reflected waves," IEEE J. Quantum Electron. **15**, 3 (1979).
5. E. Patzak, H. Olesen, A. Sugimura, S. Saito, and T. Mukai, "Spectral linewidth reduction in semiconductor lasers by an external cavity with weak optical feedback," Electron. Lett. **19**, 22 (1983).
6. D. Arsenijević, M. Kleinert and D. Bimberg, "Phase noise and jitter reduction by optical feedback on passively mode-locked quantum-dot lasers," Appl. Phys. Lett. **103**, 231101 (2013).
7. L. C. Jaurigue, O. Nikiforov, E. Schöll, S. Breuer and K. Lüdge, "Dynamics of a passively mode-locked semiconductor laser subject to dual-cavity optical feedback," Phys. Rev. E **93**, 2 (2016).
8. K. Kobayashi, "Improvements in direct pulse code modulation of semiconductor lasers by optical feedback," IEICE Trans. E**59**, 12 (1976).
9. G. Giacomelli, M. Calzavara and F. T. Arecchi, "Instabilities in a semiconductor laser with delayed optoelectronic feedback," Opt. Commun. **74**, 1,2 (1989).
10. S. Tang and J. M. Liu, "Chaotic pulsing and quasi-periodic route to chaos in a semiconductor laser with delayed opto-electronic feedback," IEEE J. Quantum Electron. **37**, 3 (2001).
11. S. Rajesh and V.M. Nandakumaran, "Control of bistability in a directly modulated semiconductor laser using delayed optoelectronic feedback," Physica D **213**, 113 (2006).
12. F. Albert, C. Hopfmann, S. Reitzenstein, C. Schneider, S. Höfling, L. Worschech, M. Kamp, W. Kinzel, A. Forchel, and I. Kanter, "Observing chaos for quantum-dot microlasers with external feedback," Nat. Commun. **2**, 366 (2011).
13. C. Hopfmann, F. Albert, C. Schneider, S. Höfling, M. Kamp, A. Forchel, I. Kantner, and S. Reitzenstein, "Nonlinear emission characteristics of quantum dot–micropillar lasers in the presence of polarized optical feedback," New J. Phys. **15**, 025030 (2013).
14. C. Kistner, S. Reitzenstein, C. Schneider, S. Höfling and A. Forchel, "Resonantly probing micropillar cavity modes by photocurrent spectroscopy", Appl. Phys. Lett. **94,** 221103 (2009).
15. P. Gold, M. Gschrey, C. Schneider, S. Höfling, A. Forchel, M. Kamp and S. Reitzenstein, "Single quantum dot photocurrent spectroscopy in the cavity quantum electrodynamics regime," Phys. Rev. B **86,** 161301(R) (2012).
16. E. Stock, F. Albert, C. Hopfmann, M. Lermer, C. Schneider, S. Höfling, A. Forchel, M. Kamp, and S. Reitzenstein, "On-Chip Quantum Optics with Quantum Dot Microcavities," Adv. Mater. **25**, 707 (2013).
17. P. Munnelly, T. Heindel, M. M. Karow, S. Höfling, M. Kamp, C. Schneider, and S. Reitzenstein, "A pulsed nonclassical light source driven by an integrated electrically triggered quantum dot microlaser," IEEE J. Sel. Top. Quantum Electron. **21**, 681 (2015).
18. M. M. Karow, P. Munnelly, T. Heindel, M. Kamp, S. Höfling, C. Schneider, and S. Reitzenstein, "On-chip light detection using monolithically integrated quantum dot micropillars," Appl. Phys. Lett. **108**, 081110 (2016).
19. C. Böckler, S. Reitzenstein, C. Kistner, R. Debusmann, A. Löffler, T. Kida, S. Höfling, A. Forchel, L. Grenouillet, J. Claudon and J. M. Gérard, "Electrically driven high-Q quantum dot-micropillar cavities," Appl. Phys. Lett. **92**, 091107 (2008).
20. Y. C. Kouomou, P. Colet, L. Larger, and N. Gastaud, "Chaotic breathers in delayed electro-optical systems," Phys. Rev. Lett. **95**, 203903 (2005).
21. K. Al-Naimee, F. Marino, M. Ciszak, R. Meucci, and F. T. Arecchi, "Chaotic spiking and incomplete homoclinic scenarios in semiconductor lasers with optoelectronic feedback," New J. Phys. **11**, 073022 (2009).
22. E.A. Viktorov and T. Erneux, "Self-sustained pulsations in a quantum-dot laser," Phys. Rev. E **90**, 052914 (2014).
23. J. P. Reithmaier, G. Sęk, A. Löffler, C. Hofmann, S. Kuhn, S. Reitzenstein, L.V. Keldysh, V. D. Kulakovskii, T. L. Reinecke and A. Forchel, "Strong coupling in a single quantum dot–semiconductor microcavity system," Nature **432**, 197 (2004).
24. M. Sciamanna and K. A. Shore, "Physics and applications of laser diode chaos," Nat. Photonics **9**, 151 (2015).
25. S. Tang, R. Vicente, M. C. Chiang, C. R. Mirasso and J.-M. Liu, "Nonlinear dynamics of semiconductor lasers with mutual optoelectronic coupling ," IEEE J. Sel. Top. Quantum Electron. **10**, 5 (2004).
26. F. Albert, C. Hopfmann, A. Eberspächer, F. Arnold, M. Emmerling, C. Schneider, S. Höfling, A. Forchel, M. Kamp, J. Wiersig and S. Reitzenstein, "Directional whispering gallery mode emission from Limaçon-shaped electrically pumped quantum dot micropillar lasers," Appl. Phys. Lett. **101**, 021116 (2012)